Lattice Boltzmann Simulations of Single Bubble Deformation and Breakup in a Shear Flow

Yi. kun. Wei[1,*], Yuehong. Qian[1] and Hui. Xu[2]
[1]Shanghai Institute of Applied Mathematics and Mechanics, Shanghai University, Yanchang road 149#, 200072 Shanghai, China
[2]Institut Jean le Rond d Alembert, UMR CNRS 7190, Universit Pierre et Marie Curie - Paris 6, 4 Place Jussieu case 162 Tour 55-65, 75252 Paris, Cedex 05, France

Received: 8 June 2011, Accepted: 7 January 2012

Abstract:
Lattice Boltzmann method (LBM) is used to simulate the deformation and breakup of single bubble in a shear flow. Numerical simulations of single bubble deformation are qualitatively compared with experimental results in a shear flow. Respectively the rotation angle θ is quantitatively compared with experimental results according to different capillary numbers (Ca), which shows numerical simulations are in agreement with the experimental results and theoretical results. Finally, the breakup process of single bubble in a shear flow is simulated straightforwardly.

Keyword: Single bubble deformation; Shear flow; Bubble breakup; Lattice Boltzmann method; Capillary number

1. INTRODUCTION

The deformation or breakup of a bubble is a very complicated, non-linear and non-stationary hydrodynamic process in a viscous shear flow. The process is usually accompanied by a significant deformation of a bubble, indicating a complex interplay among fluid convection, viscosity and surface tension [1, 2]. The breakup of single bubble is achieved at Ca in the range of 30–45 in experiments [1]. The deformation or breakup of bubble is closely related to Ca and viscosity ratios. Breakup of bubble is found to be different from drop breakup in two distinct ways: (1) even though a surfactant free system is used tip breakup occurred; (2) no clear distinction between tip breakup and total fracture is found for bubbles [1]. In sum, breakup process of single bubble is very complex dynamics. Especially, it is a challenge for the experiment of high viscosity ratios [1].

A computational study of dynamics of a bubble rising in a viscous liquid is presented. The proposed numerical method is used to simulate a wide range of flow regimes, accurately capturing the shape of the deforming interface of the bubble and the effect of surface tension, while maintaining a good mass conservation [2]. Ogu and Prosperetti perform boundary-integral potential-flow calculations of bubble growth at outlet of a needle [3, 4]. The deformation of single bubble is simulated in these papers [5, 6]. Breakup process of bubble is a very complicated and non-stationary hydrodynamic process [7]. Numerical simulations of bubble breakup are a challenge for mathematics method (macroscopic approach, e.g. finite element method, finite different method). Mesoscopic methods such as LBM can be useful for this problem. LBM has become an established numerical approach in computational fluid dynamics [8–11].

In this paper we mainly investigate two-dimensional numerical simulations of deformation and breakup of single bubble in a shear flow. We introduce a new LBM for two-phase flows with large density ratio [12]. One can find that numerical simulations are in qualitative and quantitative agreement with experimental results. Finally, the breakup process of single bubble in a shear flow is simulated.

2. LATTICE BOLTZMANN METHOD

The LBM most widely used is lattice Bhatnagar–Gross–Krook single-relaxation-time model. We use the LB equation with a (BGK) collision term,

*Corresponding Author
Email Address: wwyk123456@hotmail.com

$$f_k(x + c_k\Delta t, t + \Delta t) = f_k(x,t) + (f_k^{eq}(x,t)) - f_k(x,t)) / \tau + \Delta f_k \tag{1}$$

where f_k is the particle density distribution function with given velocity c_k and the collision time τ. k is the index of discrete velocity Δf_k is a fictitious forcing term describing interactions between neighboring sites, this term will be specified later. c_k is the discrete velocity by the following choice:

$$c_k = \begin{cases} 0, k = 0 \\ \left(\cos\dfrac{(k-1)\pi}{2}, \sin\dfrac{(k-1)\pi}{2}\right), k = 1,2,3,4 \\ \sqrt{2}\left(\cos\left[\dfrac{(k-5)\pi}{2} + \dfrac{\pi}{4}\right], \sin\left[\dfrac{(k-5)\pi}{2} + \dfrac{\pi}{4}\right]\right), k = 5,6,7,8 \end{cases} \tag{2}$$

It is sufficient to choose the equilibrium distribution function as:

$$f_k^{eq} = \rho\omega_k\left[1 + \frac{c_{k\alpha}u_\alpha}{c_s^2} + \frac{c_{k\alpha}c_{k\beta}u_\alpha u_\beta}{2c_s^4} - \frac{u^2}{2c_s^2}\right]. \tag{3}$$

Where ω_k is associated weight coeffcient. The corresponding weight coeffcients are, $\omega_0 = \frac{4}{9}$, $\omega_k = \frac{1}{9}, k = 1,2,3,4$ and $\omega_k = \frac{1}{36}, k = 5,6,7,8$. is a constant. Greek subscripts α, β denote the space directions in cartesian coordinates [13]. The density and velocity of the fluid are calculated using

$$\rho = \sum_{k=0}^{8} f_k = \sum_{k=0}^{8} f_k^{eq}, \quad \rho u = \sum_{k=0}^{8} f_k c_k = \sum_{k=0}^{8} f_k^{eq} c_k. \tag{4}$$

The body force Δf_k in the k direction can be realized by the following choice [13]:

$$\Delta f_k = f_k^{eq}(\rho, u + \Delta u) - f_k^{eq}(\rho, u) \tag{5}$$

where $\Delta u = F \cdot \Delta t / \rho$, the body force is usually equal to a difference of equilibrium distribution functions according to the mass velocity after and before the action of a force in time step at constant density ρ. In this paper we introduce a special force [13].

$$F = \frac{1}{\delta h}\left(A\sum_{k=1}^{N}\varepsilon_k\Phi^2(x + c_k)c_k + (1-2A)\Phi(x)\sum_{k=1}^{N}\varepsilon_k\Phi(x + c_k)c_k\right) \tag{6}$$

where ε_k is the interaction strength, ε_k is 1 for $k = \{1, 2, 3, 4\}$, is 1/4 for $k = \{5, 6, 7, 8\}$ [8]. A is a single free parameter. The coefficient δ is 3/2 in the model D2Q9 and h is lattice spacing. $\Phi(x)$ is a interaction potential. The special potential function is written in the form [11]:

$$\Phi(x) = \sqrt{-U(\rho, T)}. \tag{7}$$

where $U = P(\rho, T) - \rho\theta$, $P(\rho, T)$ is the equation of state. U can be rewritten as in the reduced variables [12].

$$\begin{aligned} U' &= kP'(\rho', T') - \rho'\theta' \\ &= k\left(\frac{T'}{Z_c(v' - 0.08664/Z_c)} - \frac{0.41748}{T'^{0.5}v'Z_c^2(v' + 0.08664/Z_c)}\right) - \rho'\theta' \end{aligned} \tag{8}$$

where the coefficient k is $\frac{P_c \Delta t^2}{\rho_c h^2}$, which plays an important role in the numerical stability of LBM simulations [14]. p', T', v' and Z_c are the reduced variables of pressure, temperature ,volume, the compression factor of fluids meanwhile p_c and ρ_c are the pressure and density in critical point.

The Chapman-Enskog expansion is common tool to derive the macroscopic hydrodynamic equations that correspond to specific LBM. Performing a Taylor expansion of equilibrium distribution functions, we can obtain

$$\partial_t \rho + \partial_\alpha (\rho u_\alpha) = 0 \tag{9}$$

Meanwhile, we also obtain the momentum equation

$$\partial_t (\rho u_\alpha) + \partial_\beta (\rho u_\alpha u_\beta) = -c_s^2 \partial_\alpha (\rho + H(\rho)) + \partial_\beta [v \partial_\beta (\rho u_\alpha)] + \partial_\beta [\zeta \partial_\alpha (\rho u_\beta)] \tag{10}$$

where v and ζ are shear and bulk viscosities

$$v = \frac{c_s^2}{2}(2\tau - 1), \text{ and } \zeta = v(1 - \frac{\partial H}{\partial \rho})$$

The equation of state for this model has the form:

$$P = \rho c_s^2 + H(\rho) \tag{11}$$

where H (ρ) is equal to $-\frac{c_s^2}{2}\Phi^2(\rho)$.

3. RESULTS AND DISCUSSION

The ratio of the viscosity λ, *Ca*, Reynolds number Re and the interfacial tension are important conditions of non-dimensional numbers in a simple shear flow [5]. They are given by

$$Ca = \frac{\gamma v d}{2\sigma}, \quad \mathrm{Re} = \frac{\gamma}{v}\left(\frac{d}{2}\right)^2 \tag{12}$$

where γ is imposed shear rate. d is diameter of a bubble. v is kinetic viscosity and σ is surface tension [8]. They can be written in the form:

$$\gamma = 2U_w/H, \sigma = \frac{c^2}{D+2}\int_{-\infty}^{+\infty}\sqrt{P}\,\frac{d^2\sqrt{P}}{dn^2}dn \tag{13}$$

where U_w is the speed of moving boundary. H is the breath of computational domain. p is the equation of state and D is the dimension of space.

The defined bubble has an ellipsoidal shape at low deformation. L is its major axis and B is its minor axis in a two-dimensional approach assuming an axi symmetric bubble shape in Fig 1. Respectively, θ is the rotation angle versus the principal axis of flow. The rotation angle versus the principal axis of flow θ is closely related to *Ca*. When the shear rate increases, it is clear that θ does not depend linearly on *Ca* from experimental observation. Cox (1969) published his theoretical analysis for orientation under shear flow which follows as [1]:

$$\theta = \frac{\pi}{4} - \frac{1}{2}\arctan\left(\frac{19\lambda Ca}{20}\right) \tag{14}$$

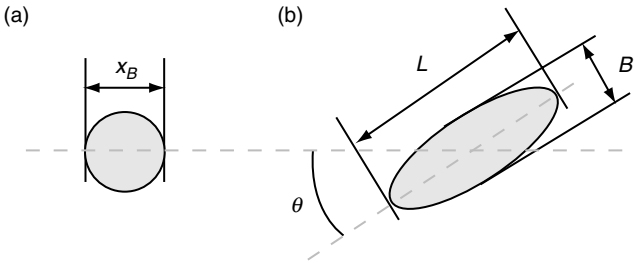

Figure 1: Parameters describing bubble deformation: x_B bubble diameter, L major axis, B minor axis, θ rotation angle. a Initial, undeformed bubble shape and b deformed bubble.

The viscosity ratio between suspended media and continuous phase is taken into account. Hinch and Acrivos (1980) proposed a model for high capillary number in systems in which the disperse phase had low viscosity compared with that of the suspending liquid [1]:

$$\theta = \arctan\left(0.359Ca^{-0.75}\right) \tag{15}$$

LBM is used to simulate dynamic behavior of a bubble in a shear fluid. As shown in Fig 2, a rectangular domain with 300×100 is considered. The domain is filled with a shear flow, and single bubble with initial radius R is placed at center of the domain. At times $t = 0$, the upper and lower walls are moved in opposite directions ($\pm$ x-directions) with a speed U_w. No-slip boundary condition is used on the moving walls, and periodic boundary condition is used on the right and left side of domain. Numerical simulations are compared with experimental results about deformation of single bubble in a shear flow in Fig 3. Values of the viscosity ratio λ and the capillary number are 0.6×10^{-7}, 0.6 in the experiment and numerical simulations [1]. It shows the typical development of bubble deformation in a shear flow in the parallel band apparatus. As soon as time evolves, the spherical bubble undergoes atransient shear deformation. The bubble changes from spherical via ellipsoidal to sigmoidal shape with pointed ends. Figure 3 (b) shows that the circular bubble gradually becomes ellipsoidal deformation in a shear flow while time is equal to 0, 200, 2000. Fig 3 clearly shows that numerical simulations are in qualitative agreement with experimental results.

The capillary number is one of most important conditions of non-dimensional numbers in a shear flow [1]. Figure 4 shows the orientation angle θ as a function of the capillary number Ca. Numerical simulations of LBM are compared with the experimental result and the slender body theory by Hinch and Acrivos [1]. The purple line is the theoretical relationship. The triangle represents experimental results and the black square is result of numerical simulations by using LBM. The values of numerical simulations are in agreement with the curve progression of experimental data and the slender body theory when the capillary number $Ca < 10$. Bubble orientation of numerical simulations is higher than experimental results in the parallel band apparatus.

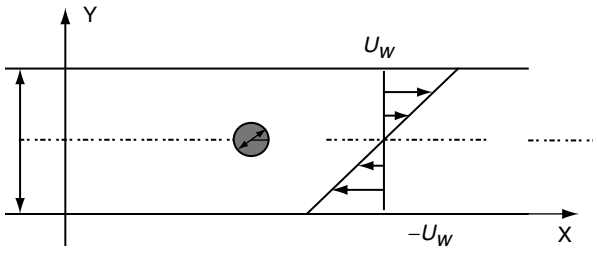

Figure 2: Sketch of the initial condition for two-dimensional bubble deformation.

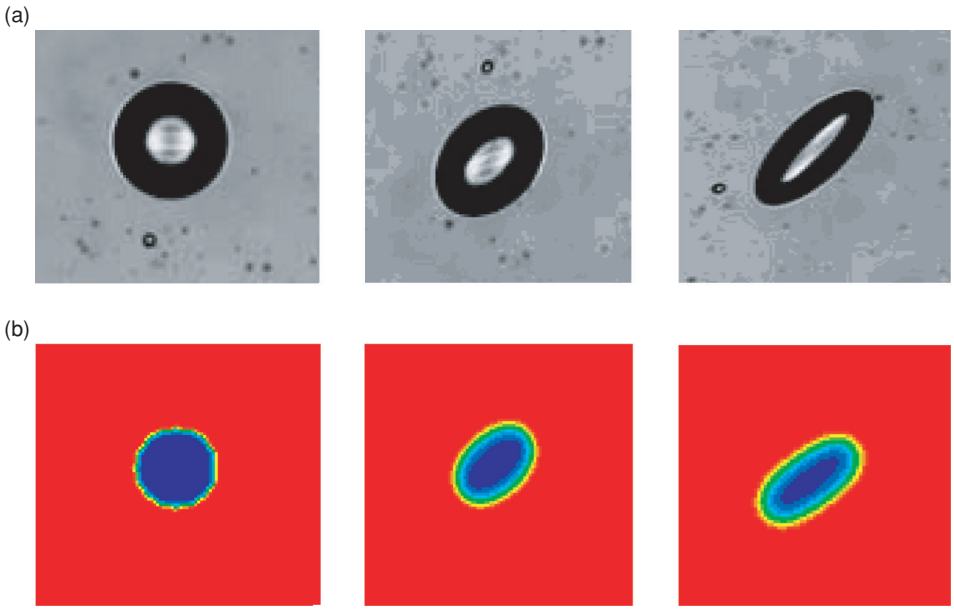

Figure 3: (a) Bubble deformation in simple shear flow as a function of elapsed time (b) the numerical simulation of lattice Boltzmann method, the radius of bubble $R = 30$, $U_w = 0.1$, $A = -0.152$.

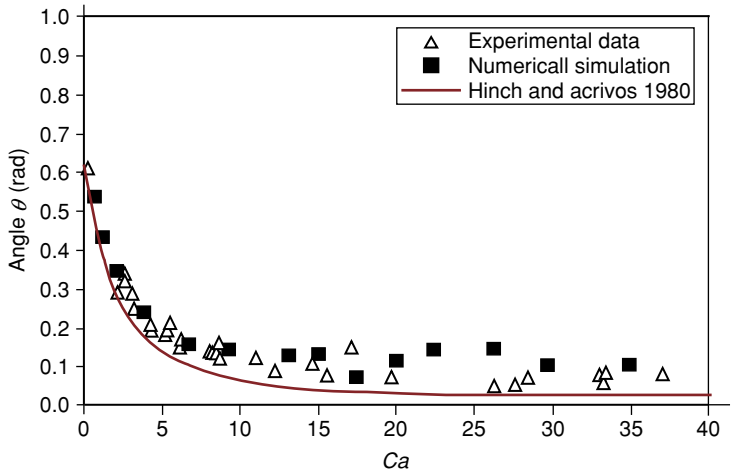

Figure 4: The orientation angle θ as a function of the capillary number Ca.

Figure 5 shows breakup process of single bubble is simulated in a shear flow. We analyze that the bubble between parallel plates is torn by shear force. We assume that value of the viscosity ratio 3×10^{-7}. Meanwhile, Ca is 35 in numerical simulations. Values of the radius of single bubble R and speed of the moving walls U_w are equal to 30 dx and 0.12. One can find that the bubble is changed and separated into two parts with progress of time. The deformed bubble (Fig. 5, b) is closed to an ellipsoidal shape with thin pointed ends. Its axis nearly aligns with the flow direction. The third picture shows the ellipsoidal bubble becomes longer in its axis direction. The fourth picture clearly shows the bubble is out of shape and pronounced beginning of tip breakup. Finally, the bubble is divided into two symmetrical and the same shape parts by shear force. Breakup process of a bubble is a very complicated kinetic process, indicating a complex interplay among fluid convection, viscosity and surface tension. Breakup of a bubble is separated into many unsymmetrical parts in a shear flow in experiment [1].

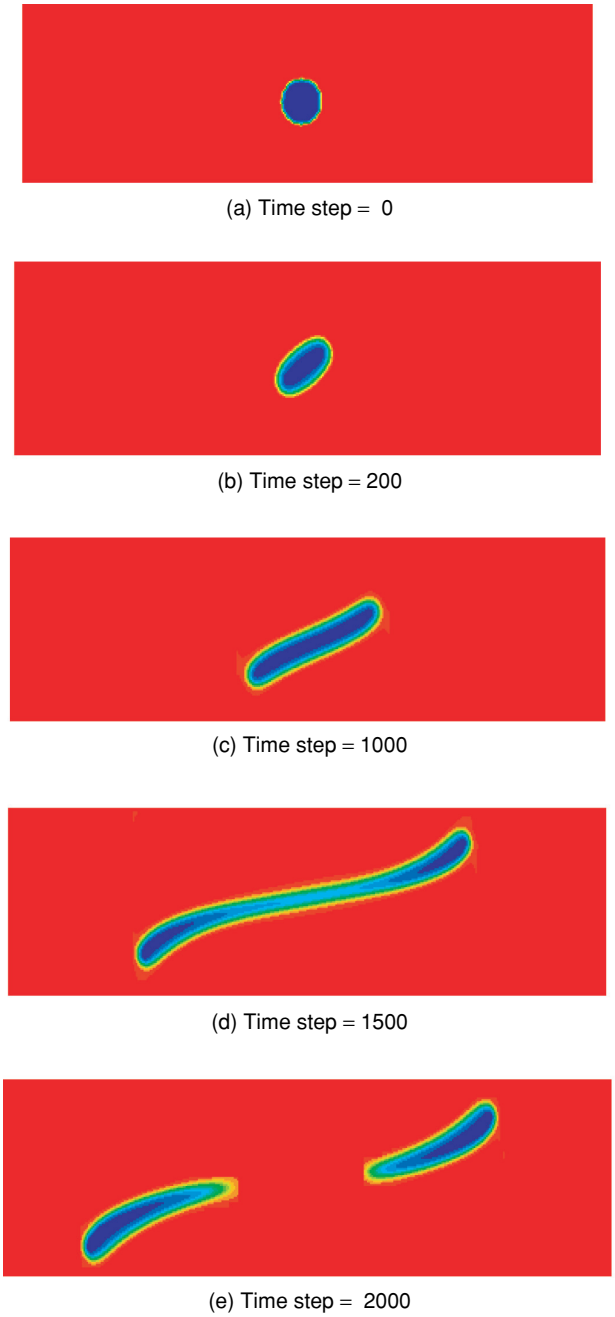

Figure 5: The breakup process of single bubble in a shear flow, the radius of bubble $R = 30$, $U_w = 0.12$, $A = -0.152$.

4. CONCLUSIONS

We mainly investigate LBM is used to simulate the deformation or breakup of single bubble in a shear flow. Numerical simulations of single bubble deformation are quantitatively compared with experimental results in a shear flow. Respectively the rotation angle θ of numerical simulations is qualitatively compared with the experimental results according to different Ca. It is shown that numerical simulations are in good agreement with the experimental results. Finally, breakup process of single bubble in a shear flow is simulated straightforwardly. Breakup process of a bubble is a very complicated kinetic process, indicating a complex interplay among fluid convection, viscosity and surface tension, which is worthy to pay attention to in the future.

ACKNOWLEDGMENTS

The research is supported in part by Ministry of Education in China via project IRT0844 and Shanghai Sci and Tech. Com. Projects of (1) Leading Scientists and (2) Excellent Academic Leaders 11XD1402300.

REFERENCES:

[1] Nadina Muller-Fische. Philip Tobler. Marco Dressler. Peter Fischer. Erich J. Windhab, Single bubble deformation and breakup in simple shear flow, *Exp Fluids* (2008) 45:917–926.

[2] Anton Smolianski, Heikki Haario and Pasi Luukka Numerical Bubble Dynamics.

[3] H. N. Oguz and A. Prosperetti, Dynamics of bubble growth and detachment from a needle, *J. Fluid Mech.* **257**, 111 (1993).

[4] Géraldine Duhar and Catherine Colin, Dynamics of bubble growth and detachment in a viscous shear flow, *PHYSICS OF FLUIDS* 18, 077101 (2006).

[5] K. Terasaka and H. Tsuge, "Bubble formation at a single orifice in highly viscous liquid," *J. Chem. Eng. Jpn.* **23**, 160 (1990).

[6] H. Z. Li, Y. Mouline, and N. Midoux, "Modelling the bubble formation dynamics in non-Newtonian fluids," *Chem. Eng. Sci.* **57**, 339 (2002).

[7] D. M. Qiu and V. K. Dhir Single-Bubble Dynamics During Pool Boiling Under Low Gravity Conditions, *JOURNAL OF THERMOPHYSICS AND HEAT TRANSFER* Vol. 16, No. 3, July–September (2002).

[8] X. Shan, H. Chen, Lattice Boltzmann model for simulating flows with multiple phases and components, *Phys. Rev. E* 47 (3) (1993) 1815–1819.

[9] M.R. Swift,W.R. Osborn, J.M. Yeomans, Lattice Boltzmann simulation of nonideal fluids, *Phys. Rev. Lett.* 75 (5) (1995) 830–833.

[10] Y.H. Qian, S. Chen, Finite size effect in lattice-BGK models, International. *J. Modern Phys. C* 8 (4) (1997) 763–771.

[11] R. Zhang, H. Chen, Lattice Boltzmann method for simulations of liquid–vapor thermal flows, *Phys. Rev. E* 67 (6) (2003) 066711.

[12] Yikun. Wei, Yuehong. Qian Lattice Boltzmann Simulations for Multiphase Fluids with Redich-Kwong Equation of State **Journal of Hydrodynamics 2011, (6) p: 283–286.**

[13] Y. Qian, D. d'Humieres, and P. Lallemand, *Europhys. Lett.* 17, 479 (1992).

[14] A.L. Kupershtokh, D.A. Medvedev, D.I. Karpov, On equations of state in a lattice Boltzmann method, *Computers and Mathematics with Applications* 58 (2009) 965–974.